Apaf-1- and Caspase-8-independent apoptosis

Running title: Apaf-1- and Caspase-8-independent apoptosis

Takeshi Imao[1] and Shigekazu Nagata[1,2]

[1]Department of Medical Chemistry, Graduate School of Medicine, Kyoto University, Yoshida, Sakyo-ku, Kyoto 606-8501, Japan

[2]Core Research for Evolutional Science and Technology, Japan Science and Technology Corporation, Kyoto 606-8501, Japan

Correspondence should be addressed to:
Shigekazu Nagata,
Department of Medical Chemistry, Graduate School of Medicine, Kyoto University,
Yoshida-Konoe, Sakyo, Kyoto 606-8501, Japan
Tel: 81-75-753-9441, Fax: 81-75-753-9446,
E-mail: snagata@mfour.med.kyoto-u.ac.jp

Abstract

Two major apoptosis pathways, the mitochondrial and death receptor pathways, are well recognized. Here we established cell lines from the fetal thymus of *Apaf-1*-, *Caspase-9*-, or *Bax/Bak*-deficient mice. These cell lines were resistant to apoptosis induced by DNA-damaging agents, RNA or protein-synthesis inhibitors, or stress in the endoplasmic reticulum. However, they underwent efficient apoptosis when treated with kinase inhibitors such as staurosporine and H-89, indicating that these inhibitors induce a caspase-dependent apoptosis that is different from the mitochondrial pathway. CrmA, a Caspase-8 inhibitor, did not prevent the staurosporine-induced apoptosis of fetal thymic cell lines, suggesting that the death receptor pathway was also not involved in this process. The staurosporine-induced cell death was inhibited by okadaic acid, a serine-threonine phosphatase inhibitor, suggesting that de-phosphorylation of a pro-apoptotic molecule triggered the death process, or that phosphorylation of an anti-apoptotic molecule could block the process. Cells of various types (fetal thymocytes, bone marrows, thymocytes, and splenocytes) but not embryonic fibroblasts were sensitive to the non-canonical staurosporine-induced apoptosis, suggesting that the non-canonical apoptosis pathway is tissue-specific.

Key Words: apoptosis, kinase inhibitors, caspase, non-canonical apoptosis, tissue-specificity

Abbreviations: E, embryonic day; FADD, Fas-associated protein with death domain; FasL, Fas ligand; IFET, immortalized fetal thymocyte; MEF, mouse embryonic fibroblast; PARP, poly(ADP)ribose polymerase; TRAIL, TNF-related apoptosis-inducing ligand.

Introduction

Apoptosis serves to eliminate cells that are useless (e.g., interdigital cells, non-reactive lymphocytes) or harmful (e.g., tumor cells and auto-reactive lymphocytes). Deregulated apoptosis causes a variety of diseases. That is, a defect in apoptosis can lead to the development of tumors and autoimmune diseases, whereas an excess of apoptosis can cause organ failure (1). Two apoptotic signaling pathways have been well characterized in mammals, the death receptor and mitochondrial pathways (also known as the extrinsic and intrinsic pathways, respectively)(2-4). In the death receptor pathway, the binding of a death factor such as Fas ligand (FasL), TNF, or TNF-related apoptosis-inducing ligand (TRAIL) to its receptor triggers a signaling cascade that leads to the activation, *via* an adaptor, Fas-Associated protein with Death Domain (FADD), of a caspase cascade consisting of Caspase-8 and Caspase-3. In the mitochondrial pathway, cytotoxic insults up-regulate or activate BH3-only proteins that activate and oligomerize Bax and Bak, and the oligomerized Bcl-2 family members Bax/Bak cause the release of cytochrome *c* from mitochondria into the cytosol (5). Cytochrome *c* then forms a complex with Apaf-1, and the cytochrome *c*/Apaf-1 complex, called the apoptosome, activates Caspase-9, which in turn activates Caspase-3 (6, 7).

The role of FADD and Caspase-8 in the death receptor-induced apoptosis pathway was confirmed by the establishment of their knock-out mice (8, 9). On the other hand, conflicting reports have been published on the roles of the signaling molecules in the mitochondrial pathway. Establishing knock-out mice, Cecconi *et al.* (10), Yoshida *et al.*

(11) and Kuida *et al*. (12) originally reported that *Apaf-1* and *caspase-9* are indispensable for genotoxic agent-induced apoptosis. However, this idea was later challenged by Marsden *et al.* (13), who showed that hemopoietic cells that lack *Apaf-1* or *Caspase-9* can undergo Bcl-2-regulated Caspase-dependent apoptosis. We recently reported that staurosporine, but not etoposide, activates Caspase-3 in embryonic day (E)14.5 fetal thymocytes, in an Apaf-1-independent manner (14). Moreover, activated Caspase-3 can be detected *in situ* in the E14.5 *Apaf-1*$^{-/-}$ fetal thymus, suggesting that an *Apaf-1*-independent intrinsic apoptotic pathway exists in these cells.

Here, to characterize this *Apaf-1*-independent pathway, we established cell lines (immortalized fetal thymocytes, IFETs) from the fetal thymus of wild-type and mutant mice. The *Apaf-1*$^{-/-}$ IFETs were resistant to genotoxic agent-induced apoptosis, but staurosporine caused efficient caspase-dependent apoptosis. Neither a null mutation of *Caspase-9* nor the double-mutation of *Bax/Bak* abolished the staurosporine-induced apoptosis of IFETs. The expression of CrmA, a Caspase-8 inhibitor (15), did not inhibit the staurosporine-induced apoptosis, either, indicating that the death receptor pathway was not used in this death process. This non-canonical Apaf-1- and Caspase-8-independent apoptosis-signaling pathway triggered by staurosporine was observed in lymphoid and myeloid tissues such as fetal thymocytes and bone marrow cells, but was barely detectable in embryonic fibroblasts. Together, these results suggest the existence of a new tissue-specific apoptotic pathway that is distinct from the death receptor and mitochondrial pathways.

Results

Establishment of *Apaf-1*-null fetal thymocyte cell line. We previously observed that Caspase-3 is activated in the *Apaf-1*-null fetal thymus (14). To characterize the Apaf-1-independent apoptosis biochemically, it was essential to establish *Apaf-1*-null cell lines. Mouse fetal thymocytes were immortalized by infecting them with mouse retrovirus carrying c-*myc* and H-*ras*^{v12}, using the RetroNectin-bound virus method. Several hundreds transformants were obtained from the pair of thymic lobes of an *Apaf-1*$^{+/+}$ or *Apaf-1*$^{-/-}$ E14.5 embryo. The transformants were cloned by limiting dilution, and termed IFETs (immortalized fetal thymocytes). The targeted disruption of the *Apaf-1* gene, or deletion of its exon 5, in *Apaf-1*$^{-/-}$ IFETs was confirmed by PCR analysis of the genomic DNA (Supplementary Figure S1A).

Incubating cell lysates with cytochrome *c* and dATP activates Caspase-3 in an Apaf-1-dependent manner (16). Accordingly, when extracts of *Apaf-1*$^{+/+}$ but not *Apaf-1*$^{-/-}$ IFET were incubated with cytochrome *c* and dATP, the Caspase-3 activation was observed (Supplementary Figure S1B), confirming that Apaf-1 was functionally inactivated by the deletion of its exon 5. The *Apaf-1*$^{+/+}$ and *Apaf-1*$^{-/-}$ IFETs grew equally well, with no requirement for specific growth factors. The surface phenotype of both the *Apaf-1*$^{+/+}$ and *Apaf-1*$^{-/-}$ IFETs was Thy1.2^{+}CD25^{-}CD44^{+} (Supplementary Figure S2), although the Thy1.2 was gradually down-regulated after repeated passages. These results suggested that the IFETs established here were T- cell lineage cells at the early stage of development.

Apaf-1-independent caspase-dependent cell death induced by staurosporine. Next, the wild-type and *Apaf-1*$^{-/-}$ IFETs were treated with staurosporine or etoposide. As shown in Figure 1A, the *Apaf-1*-null mutation blocked the etoposide-induced cell death. However, it had no effect on the staurosporine-induced cell death, and more than 90% of the staurosporine-treated *Apaf-1*$^{-/-}$ IFETs died within 12 h. A low concentration (50 μM) of caspase inhibitor (Q-VD-OPh) (17) efficiently blocked the staurosporine-induced death of *Apaf-1*$^{-/-}$ as well as the wild-type IFETs (Figure 1B), although Q-VD-OPh failed to rescue the staurosporine-induced cell-cycle arrest (Supplementary Figure S3). Not only procaspase-3 but also other caspases such as procaspase-2, -7, -8 and -9 were efficiently processed into its active form upon staurosporine treatment without Apaf-1 (Figure 1C), in sharp contrast to the lack of processing of procaspases by etoposide without Apaf-1. The concentration of staurosporine required to activate Caspase-3 in *Apaf-1*$^{-/-}$ IFETs seems to be higher than that required for the wild-type IFETs, but 0.1 μM staurosporine could still activate Caspase-3 in *Apaf-1*$^{-/-}$ IFETs in a time-dependent manner (Supplementary Figure S4).

During apoptotic cell death, poly(ADP)ribose polymerase (PARP) is cleaved, and phosphatidylserine is exposed to the cell surface (18, 19). Staurosporine, but not etoposide, caused PARP processing (Figure 1C) and phosphatidylserine-exposure without Apaf-1 (Figure 1D), confirming that executor caspases were activated by staurosporine through an Apaf-1-independent mechanism.

No requirement for Caspase-9, Bax/Bak or Caspase-8 in staurosporine-induced

cell death. Caspase-8 and -9 are essential for executing the extrinsic and intrinsic pathways of apoptosis, respectively (8, 12). To examine the requirement for Caspase-9 in the staurosporine-induced activation of Caspase-3, IFETs were established from *Caspase-9*$^{-/-}$ fetal thymocytes (Supplementary Figure S1C). As expected, etoposide could not activate Caspase-3 in the absence of Caspase-9, but staurosporine readily activated Caspase-3 without Caspase-9 (Figure 2A). Accordingly, over-expression of caspase 9 in *Caspase 9*$^{-/-}$IFETs had no effect on the staurosporine induced Caspase-3 activation (data not shown). IFETs were then established from the fetal thymocytes of *Bax*$^{-/-}$*Bak*$^{-/-}$ embryos (20)(Supplementary Figure S1D). Staurosporine but not etoposide activated Caspase-3 in the *Bax*$^{-/-}$*Bak*$^{-/-}$ IFETs (Figure 2A). The release of cytochrome c is one of the major characteristics of the mitochondrial pathway of apoptosis (21). When the wild-type and *Apaf-1*$^{-/-}$ IFETs were treated with staurosporine, the release of cytochrome *c* was observed, but there was no release of cytochrome *c* in *Bax/Bak*$^{-/-}$ IFETs (Figure 2B), indicating that cytochrome *c* was not involved in the new apoptosis pathway. Accordingly, transformation of *Apaf-1*$^{-/-}$ IFETs with human Bcl-2 had no effect on the staurosporine-induced Caspase-3 activation in *Apaf-1*$^{-/-}$ IFETs (Supplementary Figure S5). These results confirmed that staurosporine could activate Caspase-3 in IFETs without the mitochondrial apoptotic pathway.

To examine the involvement of the extrinsic pathway of apoptosis in the staurosporine-induced caspase activation, *Caspase-9*$^{-/-}$ IFETs were stably transformed with CrmA, a cowpox virus protein that inhibits Caspase-1 and -8 (15). At their early developmental stage, T cells do not express Fas (22, 23). Thus, as expected, Fas was

not expressed in the *Caspase-9*$^{-/-}$ IFETs, and the IFETs were resistant to FasL-induced apoptosis (data not shown). When the *Caspase-9*$^{-/-}$ IFETs were transformed with Fas (Supplementary Figure S6), the FasL treatment efficiently activated Caspase-3, and this activation was inhibited by CrmA (Figure 2C). On the other hand, staurosporine activated Caspase-3 even in the presence of CrmA in *Caspase-9*$^{-/-}$ IFETs (Figure 2C). These results indicated that staurosporine causes a caspase-dependent cell death that does not use the mitochondrial or the death receptor pathway.

Various reagents activate Caspase-3 to induce apoptotic cell death. As shown in Figure 3, treatment of wild-type IFETs with 2.5 μg/ml tunicamycin, 3 μg/ml actinomycin D, 10 μg/ml cycloheximide, or γ-ray (5 Gy) irradiation efficiently activated Caspase-3, and the cells were dead within 48 h in most cases (data not shown). In contrast, IFETs lacking *Apaf-1,Caspase-9, or Bax/Bak* were completely resistant to the apoptosis induced by these reagents (Figure 3A-C, and 3E). Similarly, Caspase-3 was not activated when *Bax*$^{-/-}$*Bak*$^{-/-}$ IFETs were treated with γ-rays (Figure 3D). These results indicated that most apoptosis-inducing reagents, such as DNA-damaging agents and protein-synthesis and RNA-synthesis inhibitors, required the mitochondrial pathway to activate Caspase-3.

Effect of phosphatase inhibitors on the staurosporine-induced cell death.

Staurosporine is a multi-kinase inhibitor, but it also inhibits other enzymes such as ABC transporters and topoisomerase (24, 25). Thus, it is unclear whether the inhibition of a kinase or other targets led to the induction of the Apaf-1-independent apoptosis. To

address this question, we investigated whether phosphatase inhibitors suppressed the staurosporine-induced apoptosis in *Apaf-1*$^{-/-}$ IFETs. As shown in Figure 4, okadaic acid, which is a serine/threonine phosphatase inhibitor, suppressed the staurosporine-induced Caspase-3 activation (Figure 4A) and cell death in *Apaf-1*$^{-/-}$ IFETs (Figure 4B). On the other hand, sodium orthovanadate, a tyrosine phosphatase inhibitor, had only a small effect on the staurosporine-induced Caspase-3 activation and cell death in *Apaf-1*$^{-/-}$ IFETs (Figure 4A and data not shown). These results suggest that staurosporine induces Apaf-1-independent apoptosis by inhibiting a serine/threonine kinase(s); however, we cannot formally rule out the possibility that the phosphatase inhibitors simply enhanced an anti-apoptotic pathway.

To confirm that the inhibition of kinases induced apoptotic cell death, we examined the effect of various kinase inhibitors on the apoptotic cell death. We used staurosporine analogues that had different specificities for target kinases (24, 25), H-7 and its derivatives (26), and inhibitors of MAPK and PI3K signaling pathways. Among the ten staurosporine analogues tested, four (UCN-01, GF109203X, Ro31-8220, and K252a) activated Caspase-3 in *Apaf-1*$^{-/-}$ IFETs at 2.5-50 μM, while the others had no effect at least, at the same concentration (Figure 4C). The treatment of *Apaf-1*$^{-/-}$ IFETs with 1.0 mM H-7, H-8 or H-9 did not kill them, but H-8's H-89 derivative efficiently killed the *Apaf-1*$^{-/-}$ IFETs and activated Caspase-3 at 50 μM. On the other hand, none of the MAPK-PI3K inhibitors tested (U0126, SP600125, SB239063, and LY294002) activated Caspase-3 in the *Apaf-1*$^{-/-}$ IFETs (Supplementary Figure S7).

Cell-specific mitochondria death pathway-independent Caspase-3 activation by staurosporine. To examine whether the new apoptosis pathway that was independent from the death receptor and mitochondrial pathways was present in other cell types, *Apaf-1*-null embryonic fibroblasts were prepared. As shown in Figure 5A, treatment of the primary wild-type MEFs with 10 μM staurosporine generated active Caspase-3, while no active Caspase-3 was observed with *Apaf-1*$^{-/-}$ MEFs, indicating that MEFs carry only the canonical apoptotic pathway.

To examine whether the non-canonical pathway was present in adult hemopoietic and lymphoid cells, *Tie2Cre*$^{+}$*Bax*$^{fl/fl}$*Bak*$^{-/-}$ mice {Schlaeger, 2005 #5700}{Kisanuki, 2001 #5322;Takeuchi, 2005 #5305}, in which the floxed allele of the *Bax* gene was deleted in hemopoietic and endothelial cells by Cre-mediated recombination (Supplementary Figure S8A) were analyzed. Western blotting analysis showed that adult thymocytes, bone marrow cells and splenocytes from *Bax*$^{fl/fl}$*Bak*$^{-/-}$ mice at the age of 7-9 weeks contained the 21-kDa Bax. In contrast, the thymocytes, bone marrow cells, and splenocytes from the *Tie2Cre*$^{+}$*Bax*$^{fl/fl}$*Bak*$^{-/-}$ mice did not show this band (Figure 5C, 5D and 5E), indicating that the *Bax* gene was fully deleted in these cells. As expected from the null-mutation of *Bak*, the thymocytes, bone marrow cells, and splenocytes from the *Bax*$^{fl/fl}$*Bak*$^{-/-}$ mice did not carry 28 kDa Bak (Supplementary Figure S8B). Thymocytes from *Bax*$^{fl/fl}$*Bak*$^{-/-}$ mice spontaneously die, and this death process was accelerated by treating with staurosporine (Figure 5B). The lack of Bax/Bak in *Tie2Cre*$^{+}$*Bax*$^{fl/fl}$*Bak*$^{-/-}$ strongly inhibited the spontaneous death, yet staurosporine killed the *Tie2Cre*$^{+}$*Bax*$^{fl/fl}$*Bak*$^{-/-}$ thymocytes.

When the thymocytes, bone marrow cells, and splenocytes from the *Bax*$^{fl/fl}$*Bak*$^{-/-}$ mice were treated with staurosporine or etoposide, both reagents produced the active form of Caspase-3 (Figure 5C, 5D and 5E), as in wild-type fetal thymocytes. Deleting *Bax* and *Bak* in the *Tie2Cre*$^{+}$*Bax*$^{fl/fl}$*Bak*$^{-/-}$ mice completely abolished the ability of etoposide to activate Caspase-3 in these cells. On the other hand, staurosporine could still activate the Caspase-3 in the absence of *Bax* and *Bak*. These results indicated that the non-canonical apoptosis pathway is present in lymphoid and myeloid cells such as thymocytes, splenocytes and bone marrow cells, but not in fibroblasts.

Discussion

Caspase-dependent apoptotic cell death has been thought to be mediated by two pathways: the intrinsic mitochondrial pathway and the extrinsic death receptor pathway (27). Here we showed that staurosporine, a non-selective inhibitor of diverse kinases (24), could activate Caspase-3 to kill cells, *via* two different pathways. One pathway required *Apaf-1*, while the other did not. The *Apaf-1*-independent caspase activation did not require *Bax/Bak* or *Caspase-9*, and was not inhibited by Bcl-2, and occurred without the release of cytochrome *c* from mitochondria, suggesting that the mitochondrial pathway was involved in this death process. CrmA, an inhibitor of Caspase-8 (15), also had little effect on the Apaf-1-independent caspase activation, suggesting that the death receptor pathway was also not involved in this process. Recently, the activation of inflammasomes by pathogens was shown to cause the Caspase-1-dependent cell death of macrophages and dendritic cells, which is called pyroptosis (28, 29). CrmA inhibits not only Caspase-8 but also Caspase-1 (15), suggesting that the staurosporine-induced apoptotic pathway identified here was not pyroptosis.

The *Apaf-1*- and *Caspase-1/8*-independent non-canonical apoptotic pathway was activated by various kinase inhibitors, such as staurosporine, UCN-01, a staurosporine-derivative, and H-89. The activation of Caspase-3 by these kinase inhibitors was inhibited by okadaic acid, a phosphatase inhibitor. A simple idea is that growing cells carry a phosphatase(s) that leads to the activation of Caspase-3, and specific kinases prevent the phosphatase-induced Caspase-3 activation by keeping its

target phosphorylated. Phosphatase inhibitors were previously shown to inhibit the mitochondrial and death receptor pathways (30), in which phosphatases seem to increase the death-signaling that requires de-phosphorylation. Therefore, it is possible that cells carry a pro-apoptotic molecule(s) that has the potential to induce caspase-dependent apoptosis if it is not phosphorylated. Thus, a kinase(s) in growing cells may prevent the de-phosphorylation of this molecule, and kinase inhibitors block this process to generate the active pro-apoptotic molecule(s). Phosphatase inhibitors could prevent the de-phosphorylation of the pro-apoptotic molecule, or enhance an anti-apoptotic pathway such as the NF-κB pathway, by keeping the signaling molecules phosphorylated. Staurosporine, H-8, and their derivatives have different target specificities (24, 26, 31). A more detailed analysis of the death-inducing ability of various kinase inhibitors may help elucidate the non-canonical death-signaling pathway.

Staurosporine was originally found as a molecule that induces a Bcl-2-inhibitable apoptotic death, suggesting it causes cell death *via* the mitochondrial pathway (32, 33). In fact, Yoshida *et al.* (11) by preparing *Apaf-1*-deficient mice, showed that staurosporine can not activate caspase in the absence of *Apaf-1*. On the other hand, Stepczynska *et al.* (34) suggested that a mitochondria-independent pathway was responsible for the staurosporine-induced apoptosis, because a dominant-negative Caspase-9 cannot inhibit it. Manns *et al.* (35) recently claimed that a non-canonical staurosporine-induced apoptosis pathway requires Caspase-9 but not Apaf-1. In this report, we showed that staurosporine could activate caspase-dependent apoptosis *via*

two different intrinsic pathways. The first, probably present ubiquitously, is the canonical mitochondria pathway that requires Bax/Bak, Apaf-1 and Caspase-9. The second pathway does not require the components for the mitochondrial pathway, and seems to work in a cell-type-specific manner. That is, staurosporine strongly activates the second pathway in the lymphocytes, but not embryonic fibroblasts, which apparently do not express the necessary components. This cell specificity of the non-canonical intrinsic apoptotic pathway may explain the previous controversial results on staurosporine-induced cell death, which were obtained with different cell lines and tissues (11, 34, 35).

Fetal thymocytes that lacked the canonical mitochondrial apoptotic pathway, and the cell lines derived from them, efficiently underwent caspase-dependent apoptosis by staurosporine treatment, which agrees with the observation that many apoptotic cells are present in the *Apaf-1*-null E14.5 fetal thymus (14). These apoptotic cells are observed in the E14.5 but not the E17.5 fetal thymus of *Apaf-1*-null embryos. In the E14.5 fetal thymus, most of the thymocytes are at the $CD4^-CD8^-$ stage, whereas in the E17.5 or neonate thymus, most of the thymocytes are at the $CD4^+CD8^+$, $CD4^+CD8^-$, or $CD4^-CD8^+$ stage. Three major selection processes occur during thymocyte development. In one of them, β-selection, immature thymocytes that productively rearrange the gene segments of the TCRβ locus undergo proliferative expansion and mature to the $CD4^+CD8^+$ stage, while those failing to do so die by apoptosis (36). It is tempting to speculate that the non-canonical *Apaf-1*- and *Caspase-1/8*-independent apoptotic pathway is involved in the apoptosis accompanying β-selection. In any case,

staurosporine and its derivatives, in particular, UCN-01, are under clinical trial as anti-cancer drugs (37, 38). Understanding how these kinase inhibitors cause apoptotic cell death will be essential for developing efficient treatment paradigms.

Materials and Methods

Mice. C57BL/6 mice were purchased from Nippon SLC (Hamamatsu, Japan). The *Apaf-1*$^{-/-}$ (11) and *Caspase-9*$^{-/-}$ (12) mice were maintained on a C57BL/6 background, and the *Bax*$^{-/-}$*Bak*$^{-/-}$ (20, 39) and *Tie2Cre*$^{+}$*Bax*$^{fl/fl}$*Bak*$^{-/-}$ (40, 41) mice were on a mixed genetic background between C57BL/6 and 129/Sv. The mice were housed in a specific pathogen-free facility at the Kyoto University, Graduate School of Medicine, and all animal experiments were carried out in accordance with protocols approved by the Animal Care and Use Committee of the Kyoto University Graduate School of Medicine. To determine the genotype of the *Apaf-1*, *Caspase-9*, *Bax*, *Bak*, and *Tie2Cre* alleles, DNA from embryonic tissues or adult tail-snip tissue was analyzed using PCR. For *Apaf-1*, wild-type- (5'-CTCAAACACCTCCTCCACAA-3') and mutant-specific (5'-GGGCCAGCTCATTCCTC-3') sense primers were used with a common antisense primer (5'-GTCATCTGGAAGGGCAGCGA-3'). For *Caspase-9*, 5'-AGGCCAGCCACCTCCAGTTCC-3' and 5'-CAGAGATGTGTAGAGAAGCCCACT-3' for wild-type, and 5'-CGTGCTACTTCCATTTGTCACGTC-3' and 5'-ACACCCTTGCAAGTCAGAGGTATG-3'for the mutant were used. For *Bax*, wild-type- (5'-GAGCTGATCAGAACCATCATG-3') and mutant-specific (5'-CCGCTTCCATTGCTCAGCGG-3') sense primers and a common antisense primer (5'-GTTGACCAGAGTGGCGTAGG-3') were used. For the floxed allele of the *Bax* gene, wild-type- (5'-CTGGGGCGCGCGGATCCATTCCCACCG-3') and mutant-specific (5'-TACGAAGTTATTAGGTCTGAAGAGGAG-3') sense primers were used with a common antisense primer

(5’-CCCTAGTAGTGACAAGTAGCATGGAAG-3’). For *Bak*, wild-type-(5’-GGTGTCCACACTAGAGAACTACTC-3’) and mutant-specific (5’-CTATCAGGACATAGCGTTGG-3’) sense primers were used with a common antisense primer (5’-GAGCCATGAAGATGTTTAGC-3’). For the *Tie2Cre* allele, a sense primer in the *Tie2* promoter region (5’-CCCTGTGCTCAGACAGAAATGAGA-3’) was used with an antisense primer in the *Cre* coding region (5’-CGCATAACCAGTGAAACAGCATTGC-3’).

Cells, antibodies, and reagents. Mouse embryonic fibroblasts (MEFs) were prepared from E14.5 mouse embryos as previously described (42), and cultured in DMEM containing 10% FCS (Gibco, Grand Island, NY). Plat-E cells (43) were cultured in DMEM containing 10% FCS, 1 μg/ml puromycin (Clontech, Palo Alto, CA), and 10 μg/ml blasticidin S (Invitrogen, Carlsbad, CA).

Rat anti-mouse CD16/CD32 monoclonal antibody (mAb) (2.4G2) (Mouse BD Fc Block), FITC-conjugated rat anti-mouse Thy1.2 mAb (53-2.1), PE-conjugated rat anti-mouse CD25 mAb (7D4), Cy-Chrome-conjugated rat anti-mouse CD44 mAb (IM7), PE-conjugated hamster anti-mouse Fas mAb (Jo2), and mouse anti-PARP mAb (C2-10) were purchased from BD PharMingen (San Diego, CA). Rabbit monoclonal antibodies against Caspase-3 (8G10), and GAPDH (14C10), rabbit polyclonal antibodies against cleaved caspase 6, cleaved caspase 7, and mouse cleaved caspase 8 were from Cell Signaling (Danvers, MA). Rabbit anti-caspase 2 was from Abcam (Cambridge, MA), and mouse anti-caspase 9 mAb (5B4) was purchased from Medical

Biological Laboratories (Nagoya, Japan). Mouse anti-α-tubulin mAb (Ab-1) was from Calbiochem (San Diego, CA), rabbit anti-Bax (N-20) Ab and anti-Bcl-2 (C 21) Ab were Santa Cruz Biotechnology (Santa Cruz, CA), rabbit anti-Bak (NT) Ab was from Millipore (Temecula, CA), and HRP-conjugated goat anti-rabbit and anti-mouse Ig Abs were from Dako (Copenhagen, Denmark). FITC-conjugated mouse anti-cytochrome *c* mAb (6H2.B4) was purchased from BioLegend (San Diego, CA).

Leucine-zipper-tagged human FasL was prepared as previously described (44). Cytochrome *c* from bovine heart, tunicamycin, cycloheximide, etoposide, sodium orthovanadate, K252a, UCN-01, SB239063, and LY294002 were purchased from Sigma-Aldrich (St Louis, MO). Actinomycin D, 4-(2-aminoethyl)-benzenesulfonyl fluoride hydrochloride (AEBSF), and okadaic acid were from Wako Pure Chemical (Osaka, Japan). The Caspase inhibitor, Q-VD-OPh was from R & D Systems (Minneapolis, MN). GF109203X, Ro31-8220, Ro31-6045, Ro31-6233, K252c, KT5823, and H-7 were from Enzo Life Sciences (Farmingdale, NY), H-9 was from Santa Cruz, U0126 was from Promega (Madison, WI), Gö 6976 was from LC Laboratories (Woburn, MA), KT5720 and SP600125 were from Calbiochem, and H89 was obtained from Cayman Chemical (Ann Arbor, MI).

Plasmids. The pCX4pur, pCX4bsr, pCX4hyg, pCX4pur/H-*ras*^{V12}, and pCX4bsr/c-*myc* retroviral vectors (45) were provided by Dr. Tsuyoshi Akagi (KAN Research Institute, Kobe, Japan). The pCX4 vector was constructed by removing the drug selection marker. The coding sequence of mouse Fas (46) was inserted into pCX4bsr

(pCX4bsr/m*Fas*), while the coding sequence of *CrmA* (47, 48) was inserted into pCX4pur (pCX4pur/*crmA*). The human BCL-2-expression plasmid, pEF-BOS/Bcl-2 was as previously described {Itoh, 1993 #665}.

Production of retroviruses. To produce retrovirus, Plat-E cultured in DMEM containing 10% FCS was transfected with expression vector using FuGENE 6 (Roche Applied Science, Basel, Switzerland). After culturing at 37°C for 48 h, the supernatant was collected, passed through a 0.45-μm filter unit (Millipore, Billerica, MA), and centrifuged at 6,000 x *g* for 16 h at 4°C (49). After centrifugation, the pellet was re-suspended in a 1/10 original volume of the culture medium and stored at -80°C.

Establishment of immortalized fetal thymocytes. Cells from the fetal thymus were immortalized by infection with retroviruses carrying H-*ras*^{V12} and c-*myc*. That is, fetal thymocytes were cultured in the presence of IL-7 (50), then infected with retrovirus using a RetroNectin kit (Takara Bio, Shiga, Japan) coupled with centrifugation, as recommended by the supplier. In brief, the wells of a 96-well plate (flat-bottom, BD Falcon) were coated with 6 μg of RetroNectin at 4°C overnight, and then incubated at room temperature for 30 min in PBS containing 2% BSA. The retroviruses were added to the wells, and the plate was centrifuged at 2,000 x *g* for 2 h at room temperature, and washed with PBS. Primary E14.5 mouse fetal thymocytes were suspended in culture medium [DMEM containing 10% FCS, 1 x NEAA (non-essential amino acids), 50 μM 2-mercaptoethanol, 10 mM HEPES-NaOH (pH 7.4)] supplemented with 5 ng/ml

mouse IL-7 (PeproTech, Rocky Hill, NJ) and added to the wells. The cells were attached to the wells by centrifuging at 400 x *g* for 5 min, and the plate was incubated for 3 days at 37°C. E14.5 *Apaf-1*$^{+/+}$ and *Apaf-1*$^{-/-}$ fetal thymocytes were infected with retroviruses from pCX4pur/H-*ras*^{V12} and pCX4bsr/c-*myc*. Other thymocytes were infected with retroviruses from pCX4/H-*ras*^{V12} and pCX4/c-*myc*. A single clone of each genotype was obtained by limiting dilution.

Transfection of IFET. To express mouse Fas and CrmA, 1 x 10^5 IFETs in 12-well flat bottom plates were suspended in the culture medium containing retrovirus and 10 μg/ml polybrene (Sigma-Aldrich), centrifuged at 1,000 x *g* for 1 h at room temperature (51, 52), and cultured at 37°C for 24 h. Puromycin or blasticidin was added to the culture at a final concentration of 5 μg/ml or 50 μg/ml, and the cells were further incubated for 7 or 10 days, respectively. The BCL-2 expression plasmid, pEF-BOS/Bcl-2, was introduced into IFETs by electroporation together with hygromysin-resistant gene pCX4hyg, and the stable transformants were selected by culturing in the presence of 4 mg/ml hygromycin B (Wako Pure Chemicals).

FACS analysis. To examine the expression of surface antigens, 1 x 10^5 IFETs in 96-well round-bottom plates were centrifuged at 300 x *g* for 3 min at 4°C, washed with FACS staining buffer (2% FCS and 0.02% NaN_3 in PBS), pretreated with Fc block, stained with fluorescent dye-conjugated antibodies, and analyzed by FACSCalibur (BD).

To detect phosphatidylserine exposed on apoptotic cells, 6.25 x 10^4 cells were incubated at room temperature for 15 min with 500-fold diluted Cy5-conjugated Annexin V (BioVision, Mountain View, CA) in 0.5 ml of Annexin V staining buffer [10 mM HEPES-NaOH (pH 7.4), 140 mM NaCl, and 2.5 mM $CaCl_2$]. Propidium iodide (PI) was added to a final concentration of 2.5 μg/ml, and the samples were incubated at room temperature for 5 min, and analyzed by FACSCalibur (53).

Cell-free assay for Caspase-3 activation. The cytochrome *c*-induced activation of Caspase-3 was assayed essentially as described (54). In brief, IFETs were harvested by centrifugation at 400 x *g* for 5 min at 4°C, washed with extraction buffer [50 mM PIPES-KOH (pH 7.0), 20 mM KCl, 5 mM EGTA, 1 mM DTT, and 10 mM AEBSF], and suspended in 0.8 volumes of the extraction buffer. After incubation on ice for 20-30 min, the cells were disrupted in a Dounce homogenizer (Wheaton, Millville, NJ) with 100 strokes of a tight pestle. The cell lysates were subjected to centrifugation at 10,000 x *g* for 10 min at 4°C, and the supernatant was further centrifuged at 100,000 x *g* for 1 h at 4°C to obtain the S-100 fraction. Protein (100 μg) of the S-100 fraction was incubated at 37°C for 30 min with 200 μM dATP and 4 μM cytochrome *c* in 25 μl of the extraction buffer. The reaction was stopped by placing the reaction mixture on ice, and the sample was mixed with an equal volume of 2 x SDS sample buffer [125 mM Tris-HCl (pH 6.8), 4% SDS, 20% glycerol, 0.02% BPB, and 10% 2-mercaptoethanol] for Western blotting.

Assay for apoptosis. To induce apoptosis, IFETs, primary thymocytes and splenocytes, bone-marrow cells treated with erythrocyte lysis buffer, and MEF at passage 3 were suspended at 1 x 10^6, 1 x 10^7, 5 x 10^6, and 5 x 10^4 cells/ml in the culture medium, respectively, and incubated at 37°C with 10 μM staurosporine, 50 μM etoposide. To induce apoptosis by γ-rays, the cells were irradiated with 5 Gy using a ^{137}Cs gamma-irradiator (dose rate of 0.744 Gy/min in a Gammacell 40 Exactor, Nordion International, Kanata, Ontario, Canada), and incubated at 37°C. Viable cells were counted by the trypan blue exclusion assay.

Western blot analysis. Cells were harvested by centrifugation at 1,100 x *g* for 5 min at 4°C, washed with PBS, suspended at 1.0-10 x 10^7 cells /ml in RIPA buffer [50 mM Tris-HCl (pH 7.6), 150 mM NaCl, 1% NP40, 0.1% SDS, and 0.5% sodium deoxycholate] containing a protease inhibitor cocktail (cOmplete, Mini, Roche), and incubated on ice for 15 min. Samples were centrifuged at 13,000 x *g* for 15 min at 4°C. The protein concentration of the supernatant was adjusted to 0.5 mg/ml with RIPA buffer, and the sample was mixed with an equal volume of 2 x SDS sample buffer. After incubating at 98°C for 5 min, the proteins were separated by 10-20% gradient SDS–PAGE if not specified, and transferred to PVDF membranes (pore size: 0.22 μm or 0.45 μm, Millipore). After incubation at room temperature for 1 h with blocking buffer [TBST (Tris-buffered saline containing 0.05% Tween 20) supplemented with 5% non-fat dry milk], the membranes were stained with primary antibodies in blocking buffer or solution 1 (Can Get Signal Immunoreaction Enhancer Solution; Toyobo,

Osaka, Japan) at room temperature for 1 h or at 4°C overnight. After being washed with TBST, the membranes were incubated at room temperature for 1 h with HRP-conjugated secondary antibodies in blocking buffer or solution 2. The proteins recognized by the antibody were then visualized by a chemiluminescence reaction (Immobilon Western, Millipore) and detected by the LAS-4000 system (Fujifilm Co., Tokyo, Japan).

Clonogenic assay. After washing with PBS containing 0.1% BSA, IFETs were re-suspended at a final concentration of 1 x 10^6 cells/ml in pre-warmed PBS containing 0.1% BSA and 10 μM CFSE (Molecular Probes, Eugene, OR), and incubated at 37^{o}C for 10 min. The staining reaction was stopped by addition of 5 volumes of ice-cold IFET culture medium, and incubated on ice for 5 min. After washing twice with ice-cold culture media, the CFSE stained-cells were pretreated with 50 μM Q-VD-OPh for 1 h in the culture media, and further treated at 37°C for 30 min with 10 μM staurosporine in the presence of 50 μM Q-VD-OPh. The cells were then washed with ice-cold culture media, and cultured at 37°C for 2 days in the culture medium containing 50 μM Q-VD-OPh. Then, the cells were stained at room temperature for 15 min with 1:1000 diluted Cy5-Annexin V in Annexin V staining buffer, and were analyzed by FACSCalibur.

Cytochrome *c* release assay. The apoptotic cytochrome *c*-release was assayed as described previously (55). In brief, 1 x 10^5 IFETs were treated at 37°C for 2 h with 10

μM staurosporine, and treated for 5 min on ice with 50 μg/ml digitonin in 100 μl of PBS containing 100 mM KCl until >95% cells were permeabilized as assessed by trypan blue exclusion. IFETs were washed with FACS staining buffer, fixed for 20 min at room temperature with 4% paraformaldehyde in PBS, washed three times, and incubated at room temperature for 1 h in blocking buffer (PBS containing 3% BSA and 0.05% saponin). The cells were then incubated for 1 h at room temperature in 1:200 diluted FITC-conjugated anti-cytochrome *c* mAb, washed, and analyzed by FACSCalibur.

Conflict of Interest

The authors declare no conflict of interest.

Acknowledgments. We thank Dr. Tsuyoshi Akagi (KAN Research Institute, Kobe, Japan) for the pCX4 series vectors, Dr. Shin Yonehara (Graduate School of Biostudies, Kyoto University) for the *Caspase-9*$^{-/-}$ mice in a C57/B6 background, and Dr. Osamu Takeuchi (Virus Institute, Kyoto University) for the *Bax*$^{-/-}$*Bak*$^{-/-}$ *and Bax*$^{fl/fl}$*Bak*$^{-/-}$ mice, and the *Tie2-Cre* transgenic mice. We are grateful to Drs. Masamichi Ishiai and Minoru Tanaka (Radiation Biology Center, Kyoto University) for help with the γ-irradiation. We thank Ms. Makiko Fujii for secretarial assistance. This work was supported in part by Grants-in-Aid for Specially Promoted Research from the Ministry of Education, Science, Sports, and Culture in Japan. T.I. is a Research Fellow

of the Japan Society of the Promotion of Science.

Reference

1. Vaux DL, Korsmeyer SJ. Cell death in development. *Cell* 1999; **96:** 245-254.
2. Strasser A, Jost PJ, Nagata S. The many roles of FAS receptor signaling in the immune system. *Immunity* 2009; **30:** 180-192.
3. Krammer PH. CD95's deadly mission in the immune system. *Nature* 2000; **407:** 789-795.
4. Nagata S. Apoptosis by death factor. *Cell* 1997; **88:** 355-365.
5. Westphal D, Dewson G, Czabotar PE, Kluck RM. Molecular biology of Bax and Bak activation and action. *Biochim Biophys Acta* 2011; **1813:** 521-531.
6. Ow YP, Green DR, Hao Z, Mak TW. Cytochrome c: functions beyond respiration. *Nat Rev Mol Cell Biol* 2008; **9:** 532-542.
7. Riedl SJ, Salvesen GS. The apoptosome: signalling platform of cell death. *Nat Rev Mol Cell Biol* 2007; **8:** 405-413.
8. Varfolomeev EE, Schuchmann M, Luria V, Chiannikulchai N, Beckmann JS, Mett IL*, et al.* Target disruption of the mouse caspase 8 gene ablates cell death induction by the TNF receptors, Fas/Apo1, and DR3 and is lethal prenatally. *Immunity* 1998; **9:** 267-276.
9. Yeh WC, Pompa JL, McCurrach ME, Shu HB, Elia AJ, Shahinian A*, et al.* FADD: essential for embryo development and signaling from some, but not all, inducers of apoptosis. *Science* 1998; **279:** 1954-1958.
10. Cecconi F, Alvarez-Bolado G, Meyer BI, Roth KA, Gruss P. Apaf1 (CED-4 homolog) regulates programmed cell death in mammalian development. *Cell*

1998; **94:** 727-737.

11. Yoshida H, Kong YY, Yoshida R, Elia AJ, Hakem A, Hakem R*, et al.* Apaf1 is required for mitochondrial pathways of apoptosis and brain development. *Cell* 1998; **94:** 739-750.

12. Kuida K, Haydar TF, Kuan CY, Gu Y, Taya C, Karasuyama H*, et al.* Reduced apoptosis and cytochrome c-mediated caspase activation in mice lacking caspase 9. *Cell* 1998; **94:** 325-337.

13. Marsden VS, O'Connor L, O'Reilly LA, Silke J, Metcalf D, Ekert PG*, et al.* Apoptosis initiated by Bcl-2-regulated caspase activation independently of the cytochrome c/Apaf-1/caspase-9 apoptosome. *Nature* 2002; **419:** 634-637.

14. Nagasaka A, Kawane K, Yoshida H, Nagata S. Apaf-1-independent programmed cell death in mouse development. *Cell Death Differ* 2010; **17:** 931-941.

15. Zhou Q, Snipas S, Orth K, Muzio M, Dixit VM, Salvesen GS. Target protease specificity of the viral serpin CrmA. Analysis of five caspases. *J Biol Chem* 1997; **272:** 7797-7800.

16. Zou H, Li Y, Liu X, Wang X. An APAF-1.Cytochrome c multimeric complex is a functional apoptosome that activates procaspase-9. *J Biol Chem* 1999; **274:** 11549-11556.

17. Caserta TM, Smith AN, Gultice AD, Reedy MA, Brown TL. Q-VD-OPh, a broad spectrum caspase inhibitor with potent antiapoptotic properties. *Apoptosis* 2003; **8:** 345-352.

18. Fadok VA, Voelker DR, Campbell PA, Cohen JJ, Bratton DL, Henson PM. Exposure of phosphatidylserine on the surface of apoptotic lymphocytes triggers specific recognition and removal by macrophages. *J Immunol* 1992; **148:** 2207-2216.

19. Soldani C, Scovassi AI. Poly(ADP-ribose) polymerase-1 cleavage during apoptosis: an update. *Apoptosis* 2002; **7:** 321-328.

20. Lindsten T, Ross AJ, King A, Zong WX, Rathmell JC, Shiels HA*, et al.* The combined functions of proapoptotic Bcl-2 family members bak and bax are essential for normal development of multiple tissues. *Mol Cell* 2000; **6:** 1389-1399.

21. Youle R, Strasser A. The BCL-2 protein family: opposing activities that mediate cell death. *Nat Rev Mol Cell Biol* 2008; **9:** 47-59.

22. Ogasawara J, Suda T, Nagata S. Selective apoptosis of CD4 CD8 thymocytes by the anti-Fas antibody. *J Exp Med* 1995; **181:** 485-491.

23. Andjelić S, Drappa J, Lacy E, Elkon KB, Nikolić-Zugić J. The onset of Fas expression parallels the acquisition of CD8 and CD4 in fetal and adult alpha beta thymocytes. *Int Immunol* 1994; **6:** 73-79.

24. Nakano H, Omura S. Chemical biology of natural indolocarbazole products: 30 years since the discovery of staurosporine. *J Antibiot (Tokyo)* 2009; **62:** 17-26.

25. Gani OA, Engh RA. Protein kinase inhibition of clinically important staurosporine analogues. *Nat Prod Rep* 2010; **27:** 489-498.

26. Hidaka H, Kobayashi R. Pharmacology of protein kinase inhibitors. *Annu Rev*

Pharmacol Toxicol 1992; **32:** 377-397.

27. Strasser A, O'Connor L, Dixit VM. Apoptosis signaling. *Annu Rev Biochem* 2000; **69:** 217-245.

28. Miao EA, Rajan JV, Aderem A. Caspase-1-induced pyroptotic cell death. *Immunol Rev* 2011; **243:** 206-214.

29. Brodsky IE, Medzhitov R. Pyroptosis: macrophage suicide exposes hidden invaders. *Curr Biol* 2011; **21:** R72-75.

30. Chatfield K, Eastman A. Inhibitors of protein phosphatases 1 and 2A differentially prevent intrinsic and extrinsic apoptosis pathways. *Biochem Biophys Res Commun* 2004; **323:** 1313-1320.

31. Fabian MA, Biggs WH, Treiber DK, Atteridge CE, Azimioara MD, Benedetti MG*, et al.* A small molecule–kinase interaction map for clinical kinase inhibitors. *Nat Biotech* 2005; **23:** 329-336.

32. Jacobsen MD, Weil M, Raff MC. Role of Ced-3/ICE-family proteases in staurosporine-induced programmed cell death. *J Cell Biol* 1996; **133:** 1041-1051.

33. Jacobson MD, Burne JF, Raff MC. Programmed cell death and Bcl-2 protection in the absence of a nucleus. *EMBO J* 1994; **13:** 1899-1910.

34. Stepczynska A, Lauber K, Engels IH, Janssen O, Kabelitz D, Wesselborg S*, et al.* Staurosporine and conventional anticancer drugs induce overlapping, yet distinct pathways of apoptosis and caspase activation. *Oncogene* 2001; **20:** 1193-1202.

35. Manns J, Daubrawa M, Driessen S, Paasch F, Hoffmann N, Löffler A*, et al.* Triggering of a novel intrinsic apoptosis pathway by the kinase inhibitor staurosporine: activation of caspase-9 in the absence of Apaf-1. *FASEB J* 2011; **25:** 3250-3261.

36. Wiest DL, Berger MA, Carleton M. Control of early thymocyte development by the pre-T cell receptor complex: A receptor without a ligand? *Semin Immunol* 1999; **11:** 251-262.

37. Lapenna S, Giordano A. Cell cycle kinases as therapeutic targets for cancer. *Nat Rev Drug Discov* 2009; **8:** 547-566.

38. Fuse E, Kuwabara T, Sparreboom A, Sausville EA, Figg WD. Review of UCN-01 development: a lesson in the importance of clinical pharmacology. *J Clin Pharmacol* 2005; **45:** 394-403.

39. Knudson CM, Tung KS, Tourtellotte WG, Brown GA, Korsmeyer SJ. Bax-deficient mice with lymphoid hyperplasia and male germ cell death. *Science* 1995; **270:** 96-99.

40. Takeuchi O, Fisher J, Suh H, Harada H, Malynn BA, Korsmeyer SJ. Essential role of BAX,BAK in B cell homeostasis and prevention of autoimmune disease. *Proc Natl Acad Sci USA* 2005; **102:** 11272-11277.

41. Kisanuki YY, Hammer RE, Miyazaki J, Williams SC, Richardson JA, Yanagisawa M. Tie2-Cre transgenic mice: a new model for endothelial cell-lineage analysis in vivo. *Dev Biol* 2001; **230:** 230-242.

42. Okabe Y, Kawane K, Akira S, Taniguchi T, Nagata S. Toll-like

receptor-independent gene induction program activated by mammalian DNA escaped from apoptotic DNA degradation. *J Exp Med* 2005; **202:** 1333-1339.

43. Morita S, Kojima T, Kitamura T. Plat-E: an efficient and stable system for transient packaging of retroviruses. *Gene Ther* 2000; **7:** 1063-1066.

44. Shiraishi T, Suzuyama K, Okamoto H, Mineta T, Tabuchi K, Nakayama K*, et al.* Increased cytotoxicity of soluble Fas ligand by fusing isoleucine zipper motif. *Biochem Biophys Res Commun* 2004; **322:** 197-202.

45. Akagi T, Sasai K, Hanafusa H. Refractory nature of normal human diploid fibroblasts with respect to oncogene-mediated transformation. *Proc Natl Acad Sci USA* 2003; **100:** 13567-13572.

46. Watanabe-Fukunaga R, Brannan CI, Itoh N, Yonehara S, Copeland NG, Jenkins NA*, et al.* The cDNA structure, expression, and chromosomal assignment of the mouse Fas antigen. *J Immunol* 1992; **148:** 1274-1279.

47. Pickup DJ, Ink BS, Hu W, Ray CA, Joklik WK. Hemorrhage in lesions caused by cowpox virus is induced by a viral protein that is related to plasma protein inhibitors of serine proteases. *Proc Natl Acad Sci USA* 1986; **83:** 7698-7702.

48. Enari M, Hug H, Nagata S. Involvement of an ICE-like protease in Fas-mediated apoptosis. *Nature* 1995; **375:** 78-81.

49. Bowles NE, Eisensmith RC, Mohuiddin R, Pyron M, Woo SL. A simple and efficient method for the concentration and purification of recombinant retrovirus for increased hepatocyte transduction in vivo. *Hum Gene Ther* 1996; **7:** 1735-1742.

50. Watson JD, Morrissey PJ, Namen AE, Conlon PJ, Widmer MB. Effect of IL-7 on the growth of fetal thymocytes in culture. *J Immunol* 1989; **143:** 1215-1222.

51. Bunnell B, Muul L, Donahue R, Blaese R, Morgan R. High-efficiency retroviral-mediated gene transfer into human and nonhuman primate peripheral blood lymphocytes. *Proc Natl Acad Sci USA* 1995; **92:** 7739-7743.

52. Travers H, Anderson G, Gentle D, Jenkinson E, Girdlestone J. Protocols for high efficiency, stage-specific retroviral transduction of murine fetal thymocytes and thymic epithelial cells. *J Immunol Methods* 2001; **253:** 209-222.

53. Vermes I, Haanen C, Steffens-Nakken H, Reutelingsperger C. A novel assay for apoptosis. Flow cytometric detection of phosphatidylserine expression on early apoptotic cells using fluorescein labelled Annexin V. *J Immunol Methods* 1995; **184:** 39-51.

54. Genini D, Budihardjo I, Plunkett W, Wang X, Carrera CJ, Cottam HB*, et al.* Nucleotide requirements for the in vitro activation of the apoptosis protein-activating factor-1-mediated caspase pathway. *J Biol Chem* 2000; **275:** 29-34.

55. Waterhouse NJ, Trapani JA. A new quantitative assay for cytochrome c release in apoptotic cells. *Cell Death and Differ* 2003; **10:** 853-855.

Legends to Figures

Figure 1. Staurosporine-induced *Apaf-1*-independent apoptosis. (A) Apaf-1-independent cell death induced by staurosporine but not etoposide. *Apaf-1*$^{+/+}$ (+/+) and *Apaf-1*$^{-/-}$ (-/-) IFETs were cultured with 10 μM staurosporine (STS) or 50 μM etoposide (Eto). At the indicated time, living cells were counted by trypan blue exclusion assay, and expressed as a percentage of the initial cell number. The experiments were carried out independently for three times, and the average number was plotted with S.D. (bars). (B) Caspase-dependent Apaf-1-independent cell death induced by staurosporine. *Apaf-1*$^{+/+}$ (+/+) and *Apaf-1*$^{-/-}$ (-/-) IFETs were pre-treated with 50 μM Q-VD-OPh (Q) for 1 h, and cultured with or without 10 μM staurosporine (STS) and 50 μM Q-VD-OPh for the indicated times. Living cells were counted by trypan blue exclusion assay, and expressed as a percentage of the initial cell number. Experiments were performed independently for three times, and the average values were plotted with S.D. (bars). (C) *Apaf-1*-independent caspase activation by staurosporine but not etoposide. *Apaf-1*$^{+/+}$ (WT) and *Apaf-1*$^{-/-}$ IFETs were treated with 10 μM staurosporine (STS) for 2 h or 50 μM etoposide (Eto) for 6 h. Cell lysates were analyzed by Western blot with anti-Caspase-3,anti-cleaved Caspase2, anti-cleaved Caspase 6, anti-cleaved Caspase 8, anti-Caspase 9, anti-PARP or anti-α-tubulin Abs. Except for the Western blot for PARP, where the cell lysates were separated by 7.5% SDS-PAGE, the cell lysates were separated by 5-20% SDS-PAGE. Arrows indicate the pro- and activated form of Caspase, and non-cleaved (113 kDa) and cleaved PARP (85 kDa). (D) *Apaf-1*-independent PS exposure. *Apaf-1*$^{+/+}$ (WT) and *Apaf-1*$^{-/-}$ IFETs

were treated with 10 μM staurosporine (STS) for 2 h or with 50 μM etoposide (Eto) for 8 h, stained with Cy5-conjugated Annexin V and PI, and analyzed by FACS. Cells with no treatment (-) were analyzed similarly, and FACS profiles are shown at left. Numbers indicate the percentage of the cells in each quadrant.

Figure 2. No requirement for the mitochondrial or death receptor apoptosis pathway for the staurosporine-induced Caspase activation. (A) Requirement of the mitochondrial pathway for etoposide-induced but not staurosporine-induced Caspase-3 activation. Wild-type (WT), *Apaf-1*$^{-/-}$, *Caspase-9*$^{-/-}$, and *Bax*$^{-/-}$*Bak*$^{-/-}$ IFETs were treated with 10 μM staurosporine (STS) for 2 h or with 50 μM etoposide (Eto) for 6 h. The cell lysates were analyzed by Western blotting with anti-Caspase-3 or anti-tubulin Abs. Arrows indicate pro- and cleaved Caspase-3. (B) No requirement of the cytochrome *c*-release from mitochondria in the staurosporine-induced Caspase-3 activation. The wild-type, *Apaf-1*$^{-/-}$, and *Bax*$^{-/-}$*/Bak*$^{-/-}$ IFETs were treated with 10 μM staurosporine, permeabilized with digitonin, fixed with parafolmaldehyde, and stained with anti-cytochrome *c* (straight line), followed by FACS analysis. The cytochrome *c*-staining profile before the staurosporine-treatment is shown by dotted line. (C) No requirement for the death receptor pathway in the staurosporine-induced Caspase-3 activation in IFETs. Fas-*Casp9*$^{-/-}$ IFETs transformed with empty vector or CrmA were treated with 6.6 U/ml Fas ligand (FasL)(left) or with 10 μM staurosporine (STS)(right) for 2 h. The cell lysates were analyzed by Western blotting with anti-Caspase-3 and anti-α-tubulin Abs. Arrows indicate pro- and cleaved Caspase-3.

Figure 3. Requirement of the mitochondrial pathway for the tunicamycin-, actinomycin D-, cycloheximide-, and γ-ray-induced caspase activation in IFETs. Wild-type, *Apaf-1*$^{-/-}$ (A-C), *Caspase 9*$^{-/-}$ (E), or *Bax*$^{-/-}$*Bak*$^{-/-}$ (D and E) IFETs were treated with 2.5 μg/ml tunicamycin (Tun) for 6 h (A and E), 3 μg/ml actinomycin D (actD), 10 μg/ml cycloheximide (CHX) for 2 h (B and E), or 5 Gy γ-irradiation (C and D), and incubated at 37°C for 4 h. The cell lysates were analyzed by Western blotting with anti-Caspase-3 or anti-α-tubulin Abs. Arrows indicate pro- and cleaved Caspase-3.

Figure 4. Involvement of serine/threonine kinase in the staurosporine-induced Apaf-1-independent apoptosis. (A) Effect of phosphatase inhibitors on the staurosporine-induced Apaf-1-independent Caspase-3 activation. *Apaf-1*$^{-/-}$ IFETs were treated with 10 μM staurosporine (STS) and 1 μM okadaic acid (OA) or 1 mM orthovanadate (VO_4) for 2 h. The cell lysates were analyzed by Western blotting with anti-Caspase-3 or anti-α-tubulin Abs. Arrows indicate pro- and cleaved Caspase-3. (B) Effect of okadaic acid on the staurosporine-induced Apaf-1-independent cell death. *Apaf-1*$^{-/-}$ IFETs were cultured without or with 10 μM staurosporine (STS) or 1 μM okadaic acid (OA), or both. At the indicated times, living cells were counted by the trypan blue exclusion assay, and are expressed as a percentage of the initial cell number. Experiments were carried out independently for three times, and the average values are plotted with S.D. (bars). (C) Apaf-1-independent Caspase-3 activation by kinase

inhibitors. *Apaf-1*$^{-/-}$ IFETs were treated at 37°C for 2 h with 10 μM staurosporine (STS) or its derivatives [25 μM UCN-01, 50 μM GF109203X, 50 μM Ro31-6045, 50 μM Ro31-6233, 25 μM Ro31-8220, 2.5 μM K252a, 25 μM K252c, 50 μM Gö 6976, 50 μM KT5720, or 50 μM KT5823] or H-series kinase inhibitors [1 mM H7, H8, or H-9, or 50 μM H89]. The cell lysates were analyzed by Western blotting with anti-Caspase-3 or anti-α-tubulin Abs.

Figure 5. Tissue-specificity of the non-canonical apoptotic pathway. Wild-type and *Apaf-1*$^{-/-}$ embryonic fibroblasts (MEF) at passage 3 (A), and thymocytes (B and C), bone marrow cells (D) and splenocytes (E) from *Bax*$^{fl/fl}$*Bak*$^{-/-}$ or *Tie2Cre*$^{+}$*Bax*$^{fl/fl}$*Bak*$^{-/-}$ mice were treated with 10 μM staurosporine (STS) for 4 h, or 50 μM etoposide (Eto) for 7 h. In (A), (C), (D) and (E), the cell lysates were analyzed by Western blotting with anti-Caspase-3, anti-Bax, anti-tubulin, or anti-GAPDH Ab. Arrows indicate pro- and cleaved Caspase-3. In (B), at the indicated times, living cells were counted by the trypan blue exclusion assay, and are expressed as a percentage of the initial cell number. Experiments were carried out independently for three times, and the average values are plotted with S.D. (bars).

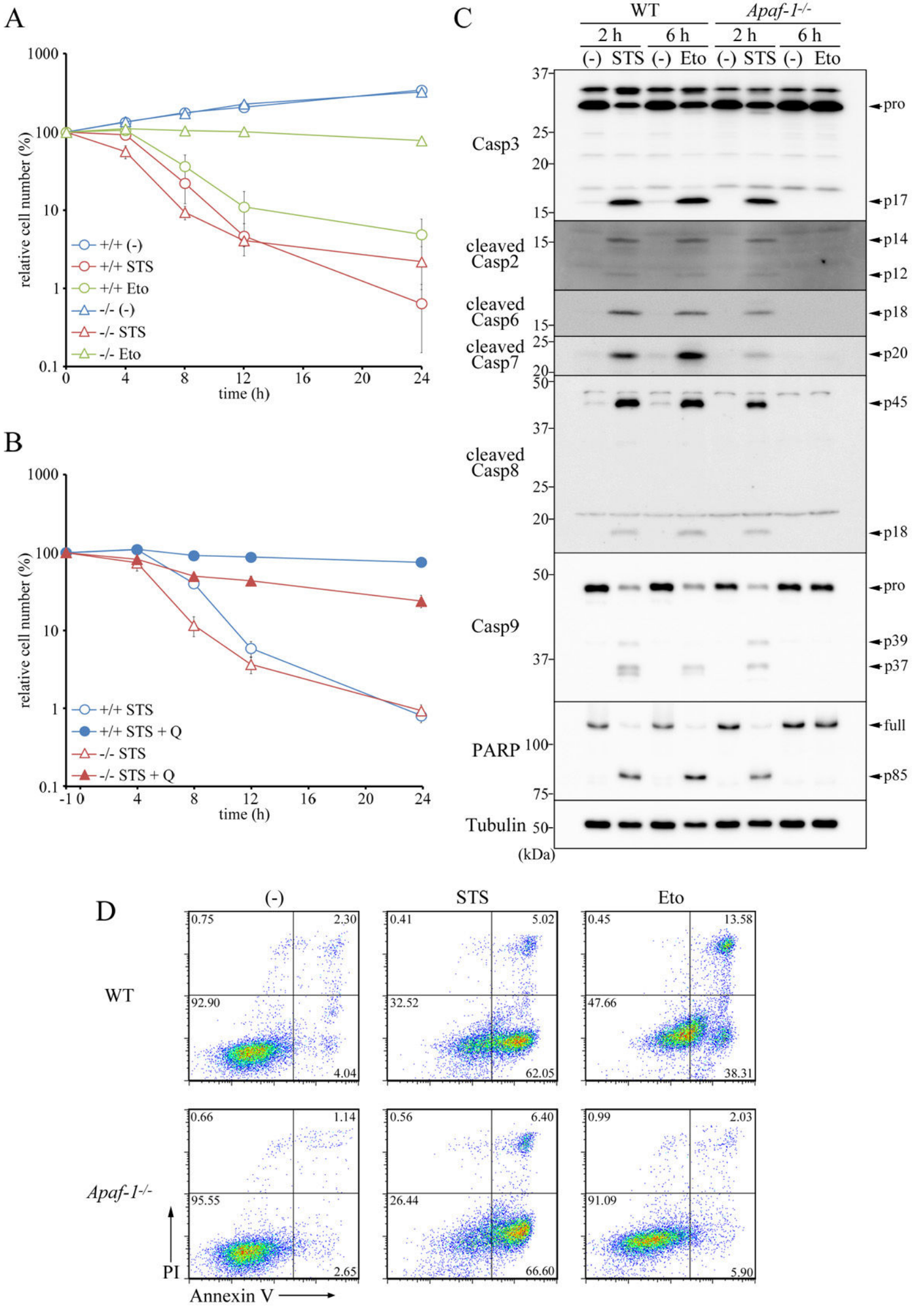

Imao et al. Fig. 1

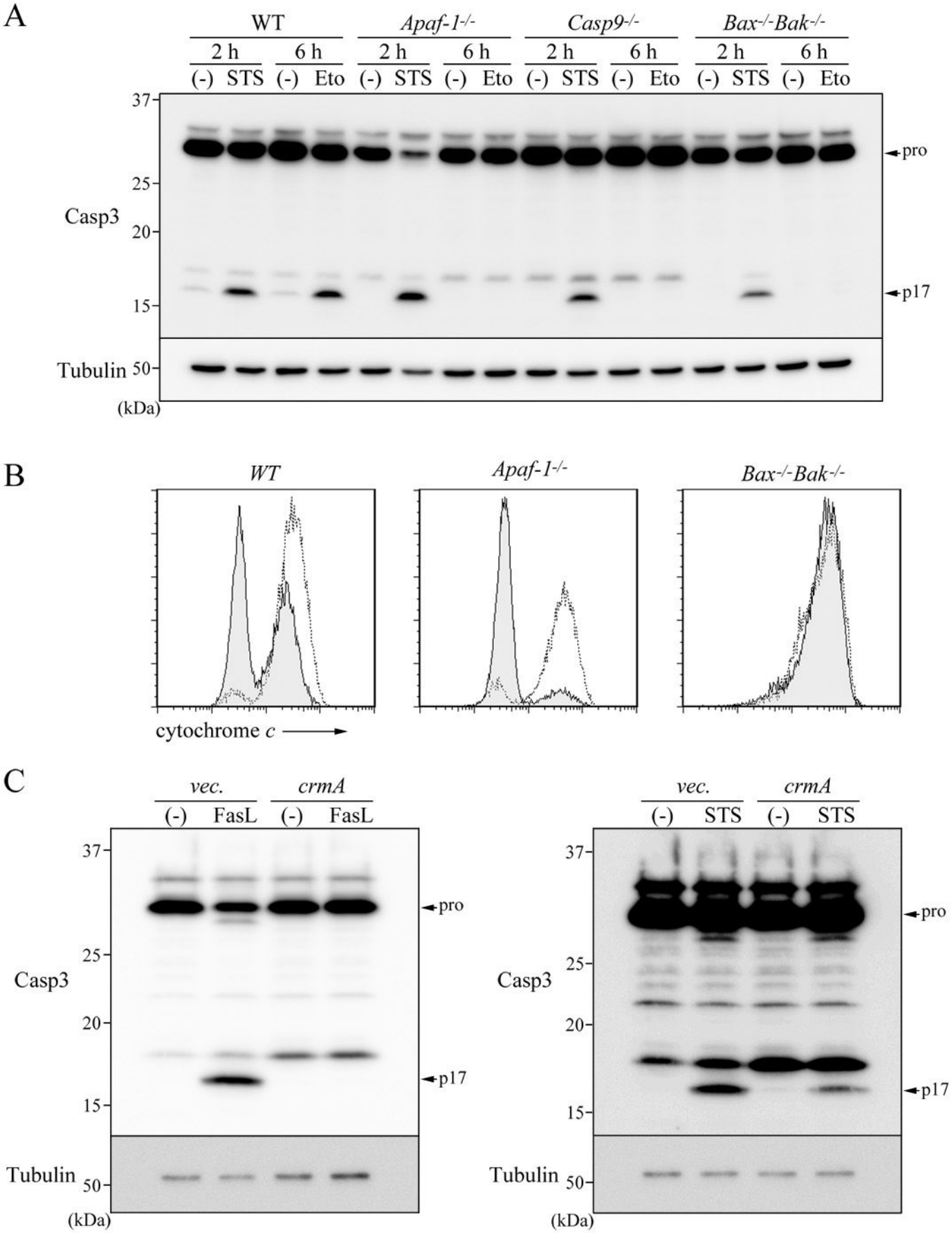

Imao et al. Fig. 2

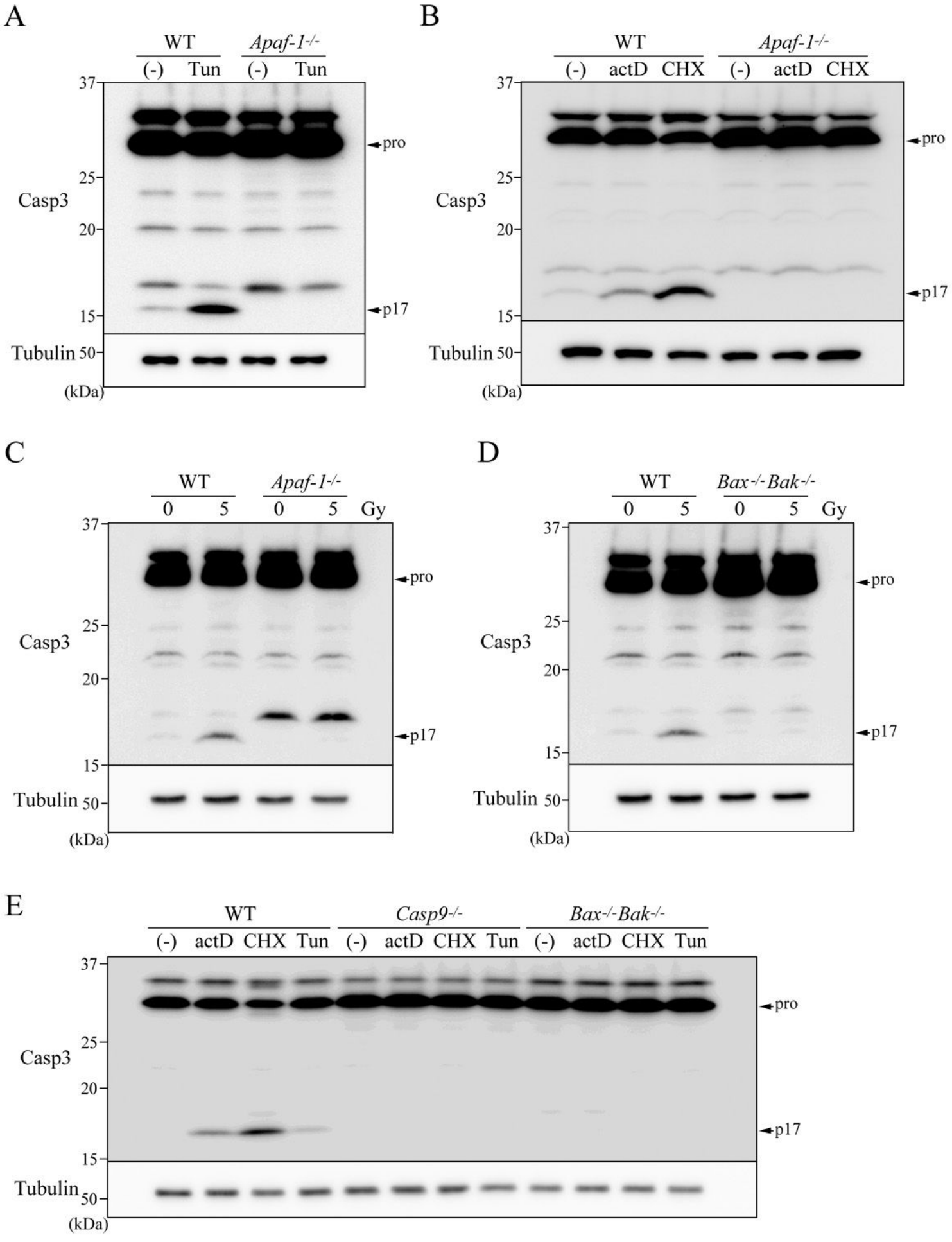

Imao et al. Fig. 3

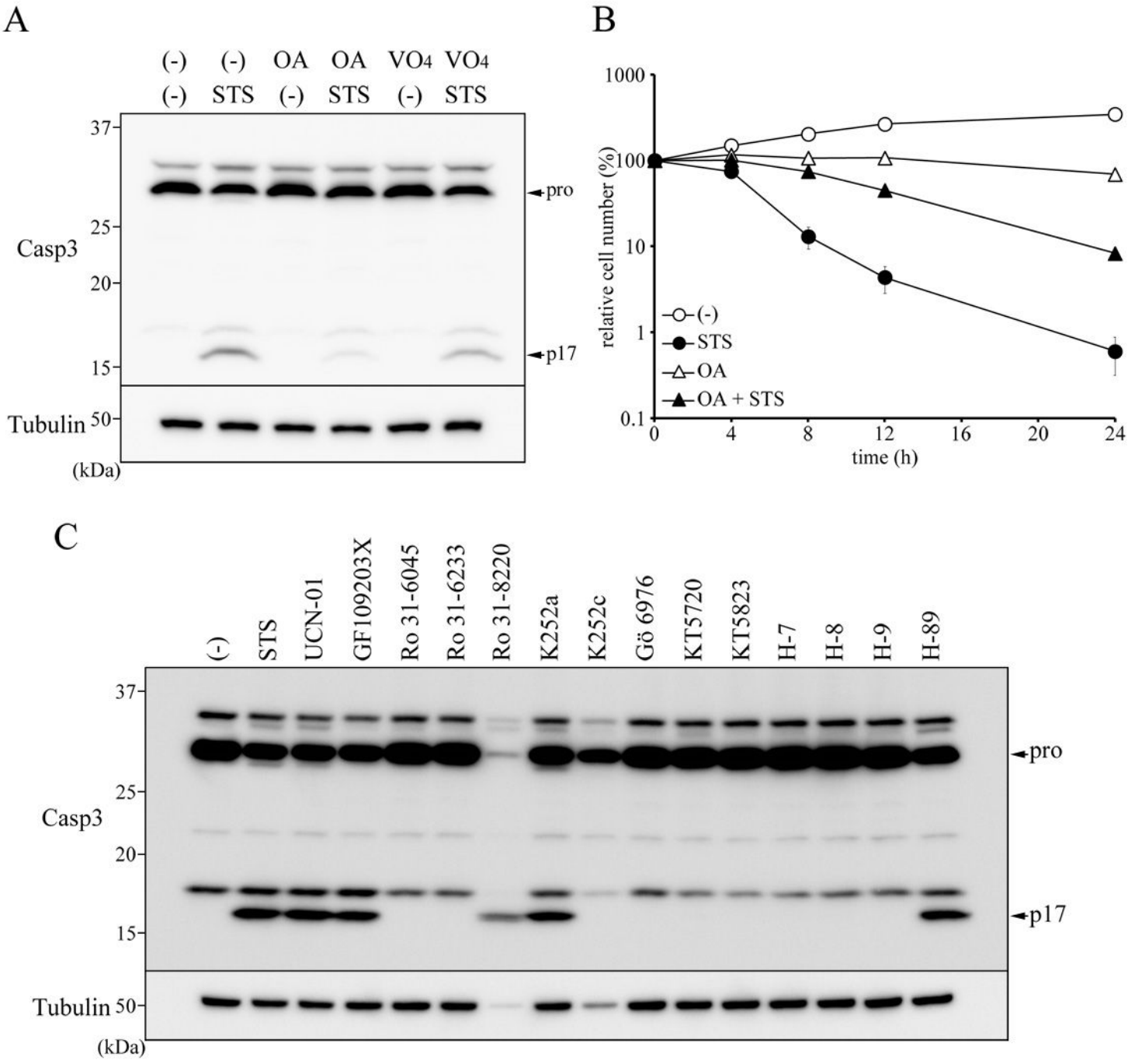

Imao et al. Fig. 4

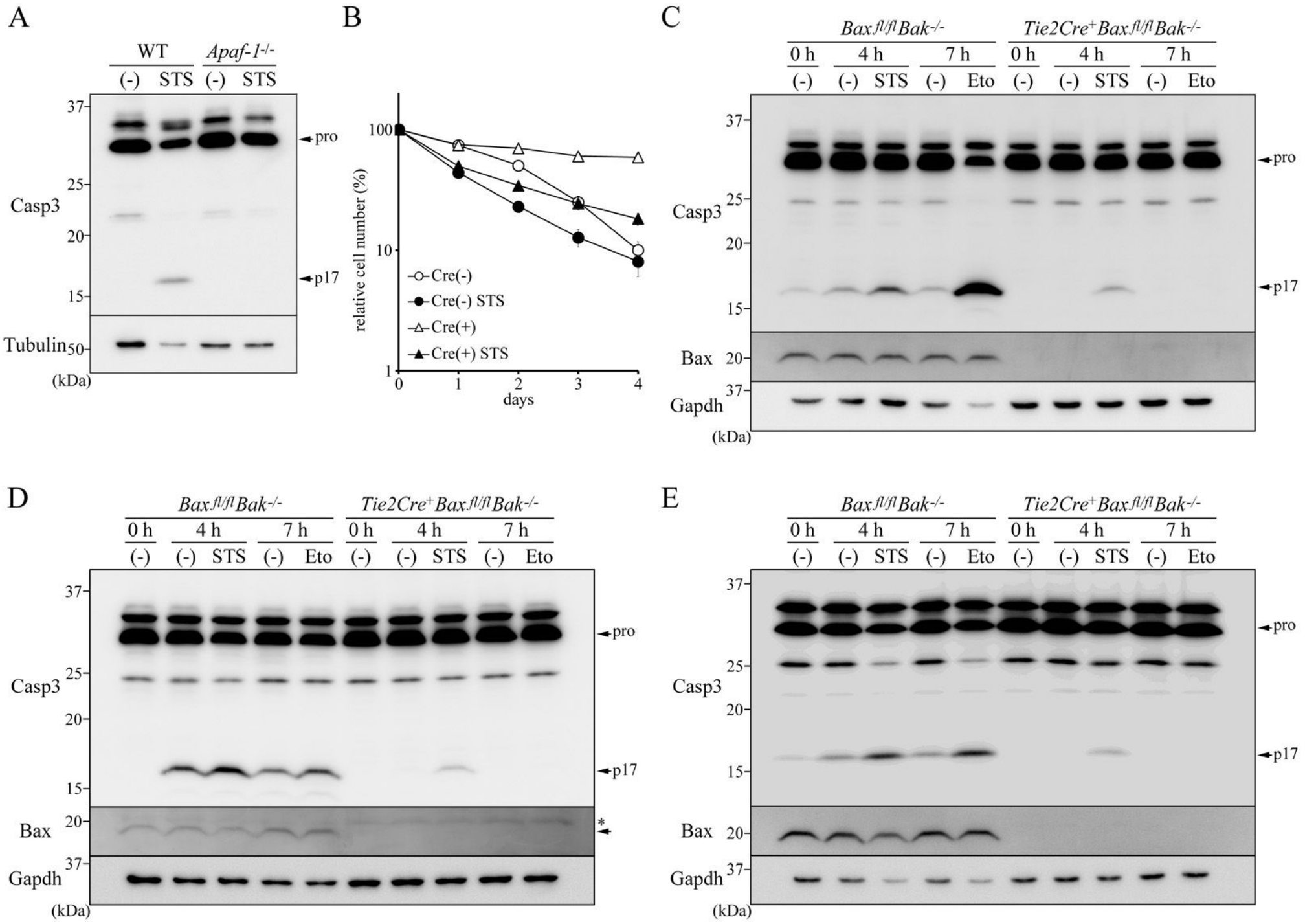

Imao et al. Fig. 5

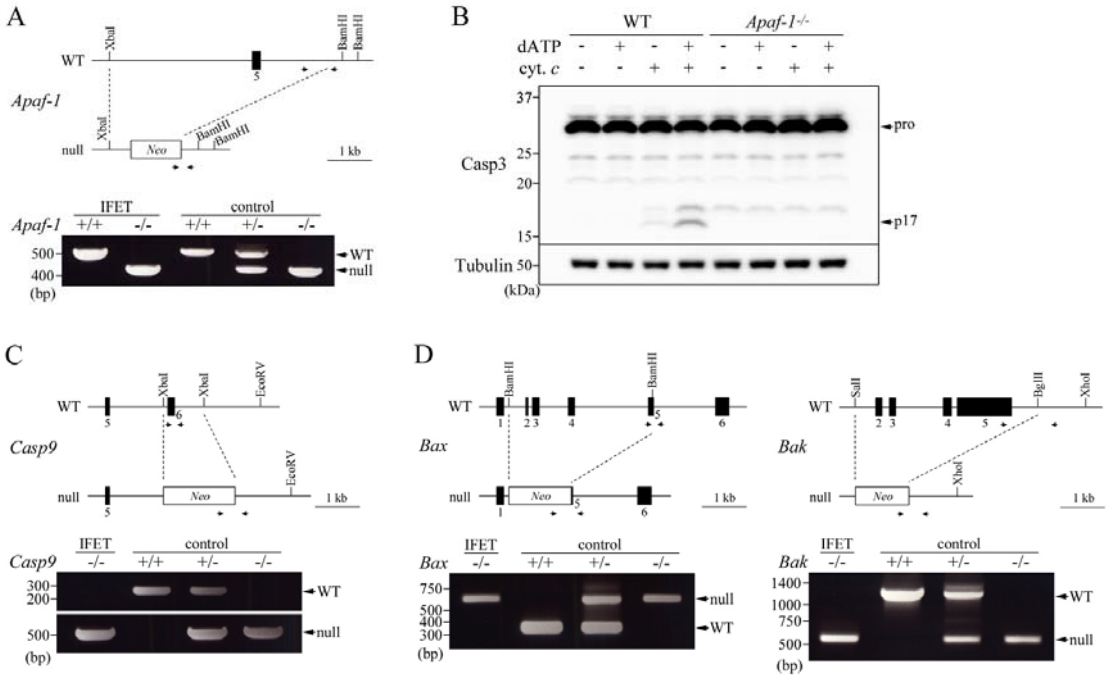

Supplementary Figure 1. Establishment of *Apaf-1*$^{-/-}$, Caspase 9$^{-/-}$, and *Bax*$^{-/-}$*Bak*$^{-/-}$ IFETs. IFETs established from *Apaf-1*$^{+/+}$ and *Apaf-1*$^{-/-}$ (A), *Caspase-9*$^{-/-}$ (C), and *Bax*$^{-/-}$*Bak*$^{-/-}$ fetal thymocytes (D) were genotyped by PCR using the primers indicated in the upper panel in each figure. DNA from *Apaf-1*$^{+/+}$, *Apaf-1*$^{+/-}$, and *Apaf-1*$^{-/-}$ (A), *Caspase-9*$^{+/+}$, *Caspase-9*$^{+/-}$, and *Caspase-9*$^{-/-}$ (C), and *Bax*$^{-/-}$*Bak*$^{-/-}$, *Bax*$^{+/-}$*Bak*$^{+/-}$, and *Bax*$^{+/+}$*Bak*$^{+/+}$ (D) mice was similarly analyzed and is shown as a control. Above the PCR data in (A), (C), and (D), the chromosomal gene structure of wild-type and null alleles was schematically drawn, in which exons and neomycin-resistant gene (Neo) are indicated by black and white boxes, respectively, and major recognition sites for restriction enzymes are shown. In (B), Proteins of the S-100 fraction were incubated at 37°C for 30 min with or without dATP and cytochrome *c,* separated by 10-20% gradient SDS-PAGE, and analyzed by Western blotting with an anti-Caspase-3 or anti-α-tubulin antibody. Arrows indicate pro- and cleaved Caspase-3.

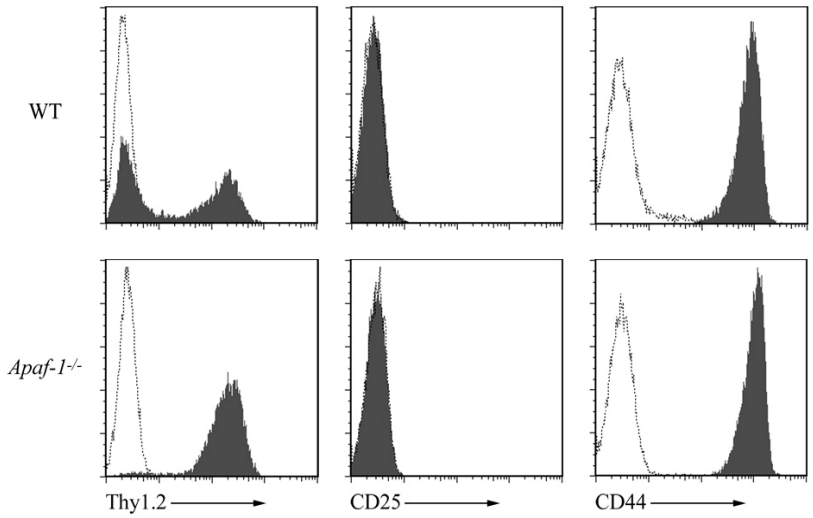

Supplementary Figure 2. Phenotype of IFETs. *Apaf-1*$^{+/+}$ and *Apaf-1*$^{-/-}$ IFETs were stained with FITC-conjugated anti-Thy1.2, PE-conjugated anti-CD25, or Cy-Chrome-conjugated anti-CD44 antibodies, and analyzed by flow cytometry (filled area). Profiles of non-stained cells are shown in open area.

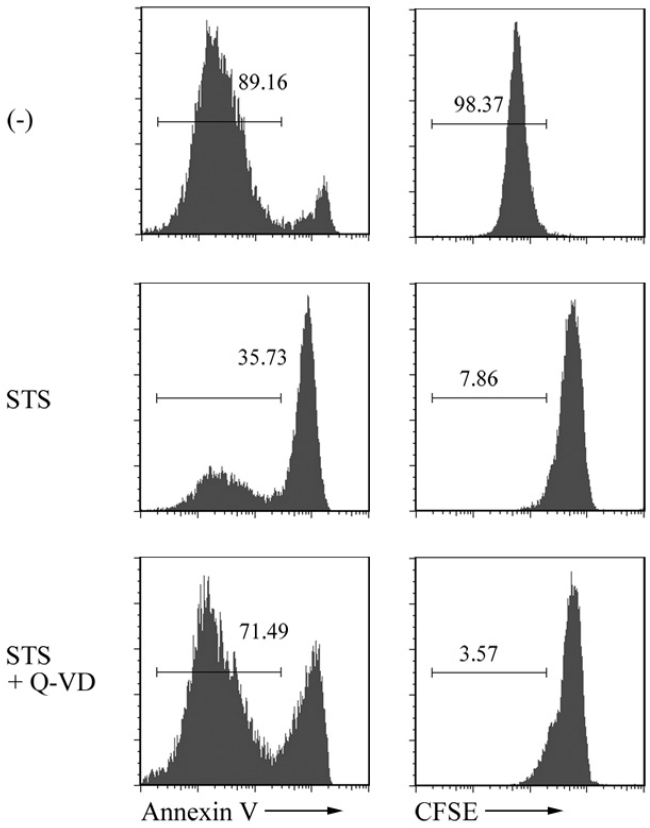

Supplementary Figure 3. No effect of caspase inhibitor on the clonogenicity of IFETs treated with staurosporine. The CFSE-labelled *Bax*$^{-/-}$*Bak*$^{-/-}$ IFETs were cultured in the absence or presence of Q-VD-OPh, and treated with 10 μM staurosporine (STS) for 30 min. The cells were further cultured for 2 days in medium with or without Q-VD-OPh, stained with Annexin V-Cy5, and analyzed by FACSCalibur for CFSE and Annexin V.

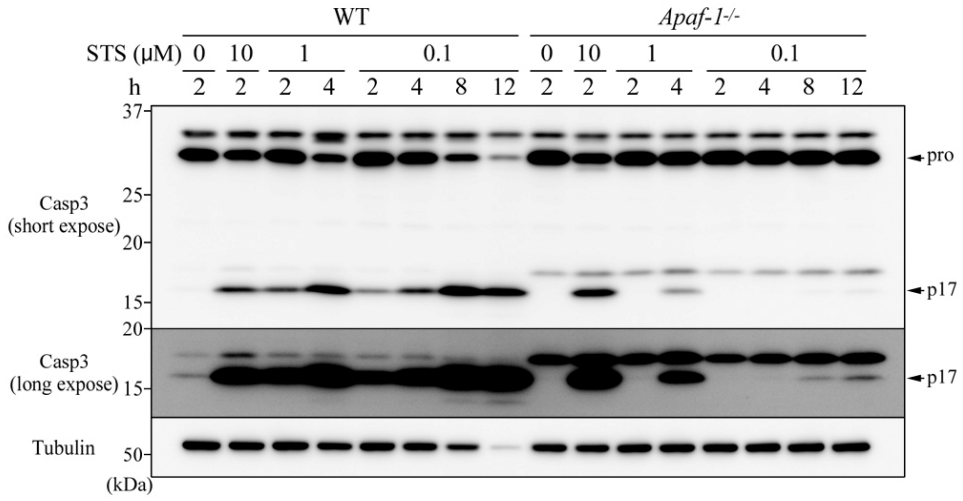

Supplementary Figure 4. Time- and dose-dependent Caspase-3-activation by staurosporine. The wild-type and *Apaf-1*$^{-/-}$ IFETs were treated with 10, 1.0, and 0.1 μM staurosporine (STS) for the indicated times, and the cell lysates were analyzed by Western blotting with anti-Caspase-3 and anti-α-tubulin Abs. Arrows indicate pro- and cleaved Caspase-3.

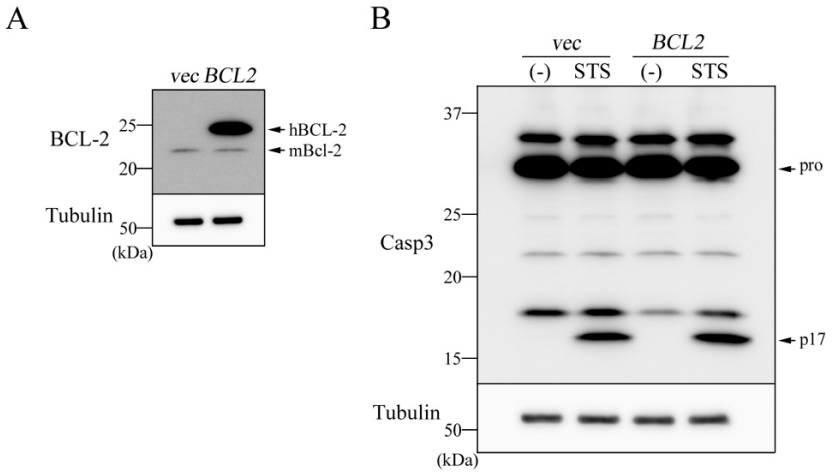

Supplementary Figure 5. No effect of Bcl-2 on the Apaf-1-independent staurosporine-induced Caspase 3-activation. *Apaf-1*$^{-/-}$ IFETs were transformed with human BCL-2, and treated with 10 μM staurosporine (STS) for 2 h. The cell lysates were analyzed by Western blotting with anti-Bcl-2, anti-Caspase-3, and anti-α-tubulin Abs. Arrows indicate human and mouse Bcl-2 (A). Pro- and cleaved Caspase-3 are indicated by arrows (B).

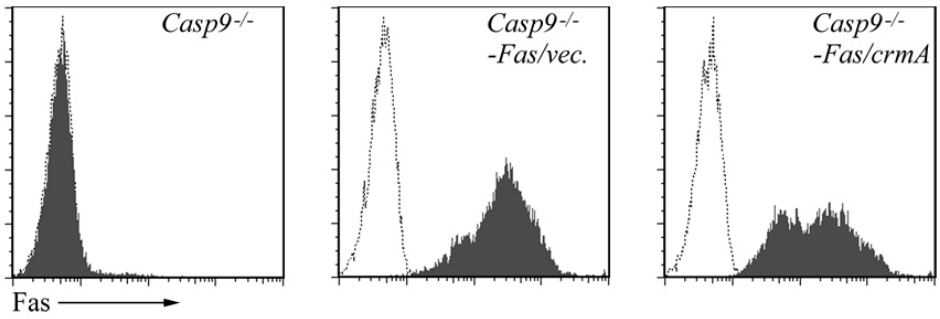

Supplementary Figure 6. Transformation of *Caspase 9*$^{-/-}$ IFETs with Fas. *Caspase-9*$^{-/-}$ IFETs were transformed with mouse *Fas,* then *crmA* or empty vector was further introduced. The cells were stained with PE-conjugated anti-mouse Fas mAb (shaded area), and analyzed by FACS. The FACS profile of non-stained cells is shown by an open area.

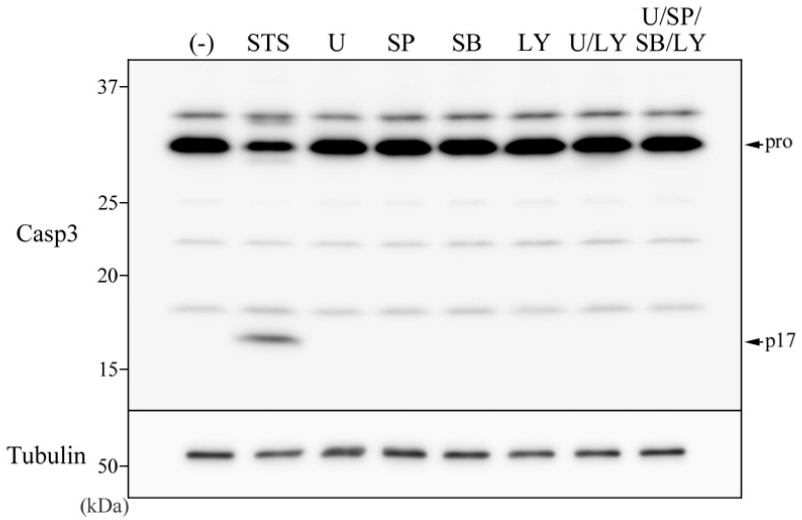

Supplementary Figure 7. No Caspase-3 activation in *Apaf-1*$^{-/-}$ IFETs by inhibitors of MAPK and PI3K pathways. The *Apaf-1*$^{-/-}$ IFET cells were treated with 10 μM staurosporine (STS), 20 μM U0126 (U), 20 μM SP600125 (SP), 20 μM SB 239063 (SB), 50 μM LY294002 (LY), 20 μM U0126 and 50 μM LY294002 (U/LY), or 20 μM U0126, 20 μM SP600125, 20 μM SB 239063, and 50 μM LY294002 (U/SP/SB/LY) for 2 h. The cell lysates were separated by 10-20% gradient SDS-PAGE, and analyzed by Western blot with anti-Caspase-3 (Top panel) and anti-α-tubulin (bottom panel) antibodies. Arrows indicate pro- and activated forms of Caspase-3.

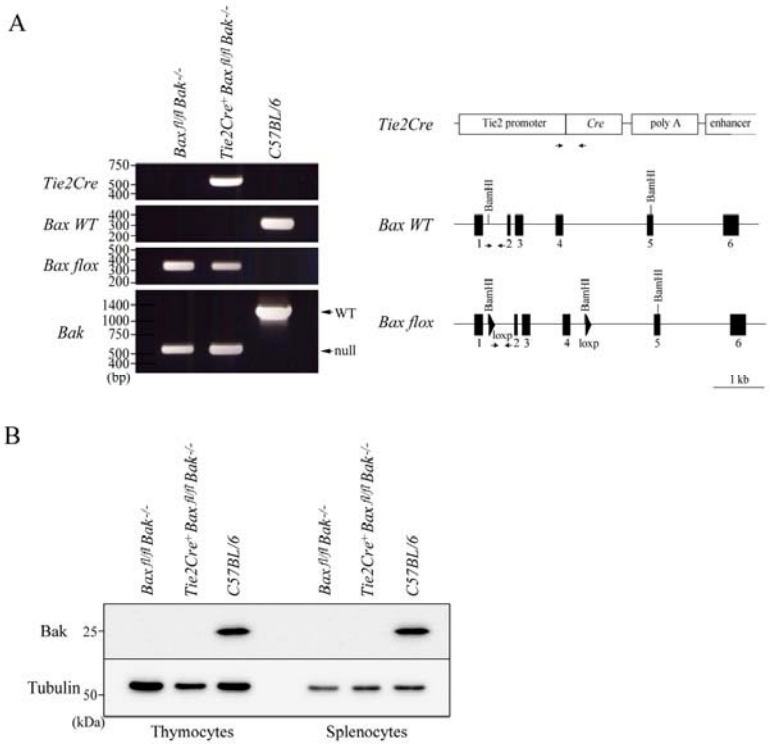

Supplementary Figure 8. Characterization of *Tie2Cre*$^{+}$*Bax*$^{fl/fl}$*Bak*$^{-/-}$ mice. (A) Genotyping. Chromosomal DNA from *Bax*$^{fl/fl}$*Bak*$^{-/-}$, *Tie2Cre*$^{+}$*Bax*$^{fl/fl}$*Bak*$^{-/-}$, and the wild-type C57BL/6 mice were analyzed by PCR for the *Tie2-Cre*, the wild-type and floxed *Bax*, the wild-type and mutant *Bak* alleles. The primes used for PCR are indicated in right. (B) No expression of Bak in *Bak*-deficient mice. The cell lysates from the thymocytes and splenocytes of *Bax*$^{fl/fl}$*Bak*$^{-/-}$, *Tie2Cre*$^{+}$*Bax*$^{fl/fl}$*Bak*$^{-/-}$, and the wild-type C57BL/6 mice were analyzed by Western blotting with anti-Bak and anti-tublin Abs.